

**Energy and density analyses of the  $1\Sigma_u$  states in the H<sub>2</sub> molecule from the united atom to dissociation.**

Journal:	<i>The Journal of Physical Chemistry</i>
Manuscript ID:	jp-2009-049395.R1
Manuscript Type:	Special Issue Article
Date Submitted by the Author:	07-Jul-2009
Complete List of Authors:	Corongiu, Giorgina; Universita' dell'Insubria, Chemistry and Enviromental Sciences Clementi, Enrico

SCHOLARONE™  
Manuscripts

1  
2  
3  
4  
5  
6  
7  
8  
9  
10  
11  
12  
13  
14  
15  
16  
17  
18  
19  
20  
21  
22  
23  
24  
25  
26  
27  
28  
29  
30  
31  
32  
33  
34  
35  
36  
37  
38  
39  
40  
41  
42  
43  
44  
45  
46  
47  
48  
49  
50  
51  
52  
53  
54  
55  
56  
57  
58  
59  
60

## Energy and density analyses of the $^1\Sigma_u^+$ states in the $H_2$ molecule from the united atom to dissociation .

Giorgina Corongiu  
Università dell'Insubria  
Dipartimento di Scienze Chimiche e Ambientali  
Via Valleggio 11, I-22100 Como, Italy

and

Enrico Clementi  
Via Carloni, 38  
I-22100 Como, Italy

**Abstract.** The  $^1\Sigma_u^+$  excited states of the  $H_2$  molecule are computed following a recent study by Corongiu and Clementi (J. Chem. Phys., in press) on the  $^1\Sigma_g^+$  states. Full Configuration Interaction computations both from Hartree-Fock molecular orbitals and Heitler-London atomic orbitals are presented and correlated with a comprehensive analysis. The basis sets utilized are either extended and optimized Slater type functions, STO, or spherical Gaussian functions, GTO.

Computations and analyses are presented for states 1 to 14, covering the internuclear distances from 0.01 to 10000 bohr. The accurate data by L. Wolniewicz and collaborators, available for the first six excited states, verify the good quality of our computations.

We focus on the characterization of the orbitals in the excited state wave functions, on the electronic density evolution from the united atom to dissociation, on quantitative decomposition of the total energy into covalent and ionic components and on detailed analyses of energy contributions to the total state energy from selected STO sub-sets.

Each manifold has one state, specifically the states 1, 3 and 6, where the second minimum has strong ionic character. State 10 dissociates into the ion pair  $H^+H^-$ .

Key words: Hydrogen molecule,  $^1\Sigma_u^+$  excited states,  $H_2$  covalent and ionic energy, dissociation products,  $H^+H^-$  ion pair, radial distribution functions, full HF-CI, full HL-CI.

1  
2  
3 **1. Introduction.** This work reports computations of the  $^1\Sigma_u^+$  excited states 1 to 14 for  
4  
5  
6 the  $H_2$  molecule, following a computational approach recently proposed [1] for a study  
7  
8  
9 on the  $^1\Sigma_g^+$  excited states. Energies of the united atom and dissociation products,  
10  
11  
12 discussions on the choice of the basis sets, details on the techniques used to analyze  
13  
14 the obtained wave functions and energies when in common both to this work and to  
15  
16 Ref. 1 are here only summarized.  
17

18  
19 The  $^1\Sigma_u^+$  excited states have been often studied [2-9]. The most accurate  
20  
21  
22 potential energy curves, PECs, for the first six states are those by Staszewska and  
23  
24 Wolniewicz [9]. Accurate computations for the first 9 states, using generalized  
25  
26 Gaussian functions, have been published by Cederbaum *et al.* [7], where, however,  
27  
28 the PECs for the states are mainly reported only graphically.  
29  
30

31  
32 In Fig. 1 the state orbital diagram for the  $^1\Sigma_u^+$  excited state manifolds reports  
33  
34 the electronic states for the united atom (He), the dissociation products for the  $H_2$   
35  
36 molecule up to  $n=4$ , i.e.  $H(1s)+H(4l)$ , the lowest state energy for the  $H_2^+$  molecular ion  
37  
38 and the lowest state energy for the  $H^+H^-$  system [1]. At the left side of Fig. 1 we  
39  
40 report the excited state energies for Helium (the united atom), the corresponding  
41  
42 designations (1 to 9) of the molecular excited states and state connexions from the  
43  
44 united atom to the  $H_2$  atomic dissociation products, namely the two atoms  $H(1s)$  and  
45  
46  $H(nl)$ , indicated in the figure with the short notation  $n=2, 3$ , and 4. The  $l$  value varies  
47  
48 from 0 to 3 (i.e. from s to f orbitals) corresponding to the excited states 1B to 9B,  
49  
50 namely up to  $n=4$ . Note that the last Helium state ( $1s7p$ ) is not connected to the right  
51  
52 site of the diagram, since the dissociation products for  $n=5$  are not reported. The  
53  
54 computations include also states with dissociation  $n=5$ , not indicated in Fig. 1.  
55  
56  
57  
58  
59  
60

In the following of this work we use both the full state notation  $nB$  with  $n=1, \dots,$   
9, or simply the short hand designation 1, ..., 9, as done in the figure, to denote

1  
2  
3 different  $^1\Sigma_u^+$  states. Computationally, these high states require very extended basis  
4 sets capable to describe from He(1s2p) up to He(1s<sup>1</sup>9p<sup>1</sup>) and He(1s<sup>1</sup>9f<sup>1</sup>) at the united  
5 atom and from H(1s) up to H(5/), with / up to 4 ,at dissociation; for this reason states  
6 10B to 14B are considered rather briefly and the corresponding computations are  
7 somewhat less reliable, being obtained with a not optimal basis sets.  
8  
9  
10  
11  
12  
13  
14  
15  
16  
17

18 **2. The  $^1\Sigma_u^+$  excited states.** The computations of the PECs start at the united  
19 atom and end at the inter-nuclear distance of  $10^4$  bohr. Two extended basis sets are  
20 used in this study: one constructed with exponential functions of Slater type, STO, the  
21 second with spherical Gaussian functions, GTO. These optimized basis sets are  
22 nearly equivalent and the computations obtained with the two types of functions yield  
23 slightly different eigen-values (and corresponding slightly different electronic  
24 densities) for a given inter-nuclear separation. The use of two different functions,  
25 STO and GTO, provides a useful numerical check and adds flexibility to the  
26 interpretation of the computations, as discussed in Ref. 1.  
27  
28  
29  
30  
31  
32  
33  
34  
35  
36  
37  
38  
39

40 The STO basis set is made by two 1s, three 2s, two 3s, one 4s, one 5s, four 2p,  
41 two 3p, one 4p,one 5p, four 3d, one 4d, one 5d, three 4f, and two 5f functions. The  
42 GTO basis set is made by 17s,10p,11d, 7f contracted to 12s, 10p, 8d and 5f. At the  
43 united atom the Helium basis set is formed by three 1s, three 2s, two 3s, two 4s, one  
44 5s , two 6s, four 2p, two 3p, two 4p, two 5p, one 6p, four 3d , one 4d, two 5d, one 6d,  
45 four 4f, three 5f and one 6f functions. With this basis set we well represent the  
46 energies of the helium singly excited states with configuration up to (1s6f). The  
47 dissociation products are well represented by the STO basis set, which accurately  
48 reproduces hydrogenic functions: in this study the hydrogenic functions have  $nl$   
49  
50  
51  
52  
53  
54  
55  
56  
57  
58  
59  
60

1  
2  
3 values ranging from  $n=1$  to  $n=5$  and  $l=0$  to  $l=3$ ; additional details on the hydrogenic  
4 functions for  $H_2$  are given in Ref. 1.  
5  
6

7  
8 In Fig. 2 the computed PECs for the  $^1\Sigma_u^+$  excited states 1B to 14B are reported.  
9  
10 The inter-nuclear separations considered in the computations are 130, precisely 25  
11 from 0.01 to 1.0 bohr, 105 from 1.0 to 100 bohr; computations at 1000 and 10000  
12 bohr are performed to define the dissociation products. In the top inset the PECs of  
13 the first 7 states are reported. In this figure the small circles represent a selected  
14 sample of energies from Wolniewicz data [9]. In the bottom inset the PECs for states  
15 7 to 14 and for  $H_2^+$  are reported. The PECs for the states dissociating into  $H(1s)$   
16 + $H(4l)$  are computed more accurately than those for the states dissociating into  $H(1s)$   
17 + $H(5l)$ , therefore the latter are considered mainly to complete the  $^1\Sigma_u^+$  state survey.  
18  
19  
20  
21  
22  
23  
24  
25  
26  
27  
28  
29  
30

31 Note for state 3B the avoided crossing with state 4B at about 5.7 bohr, and its  
32 second deep minimum at  $\sim 11$  bohr. State 6B has a shallow second minimum leading  
33 to the  $1s+4l$  dissociation limit after 100 bohr. State 7B shows a flexion point around  
34 5.6 bohr. States 8B and 9B are nearly degenerate from about 3.5 to 4.5 bohr and  
35 show an avoided crossing at  $\sim 6.1$  bohr. State 10B is very close in energy to the  $H_2^+$   
36 ground state (dashed line with circles) and from  $\sim 10$  bohr starts a slow energy  
37 decrease leading to the  $H^+H^-$  dissociation limit. States 11B to 14B lie well above the  
38 PEC of  $H_2^+$  (reported mainly to complete the  $^1\Sigma_u^+$  state manifold).  
39  
40  
41  
42  
43  
44  
45  
46  
47  
48  
49  
50

51 The accuracy of the computed energies relative to those of Wolniewicz is  
52 evident from Fig. 2. Numerically, the average deviations (in hartree) are:  $1.3 \times 10^{-4}$   
53 (with maximum deviation of  $2.3 \times 10^{-4}$  at 4.1 bohr),  $2.0 \times 10^{-5}$  (with maximum deviation  
54 of  $5.6 \times 10^{-5}$  at 1.8 bohr),  $7.2 \times 10^{-5}$  (with maximum deviation of  $1.9 \times 10^{-4}$  at 14 bohr),  
55  $2.3 \times 10^{-5}$  (with maximum deviation of  $1.1 \times 10^{-4}$  at 5.5 bohr),  $2.9 \times 10^{-5}$  (with maximum  
56 deviation of  $4.0 \times 10^{-4}$  at 1.1 bohr),  $9.6 \times 10^{-5}$  (with maximum deviation of  $2.0 \times 10^{-4}$  at 1.8  
57  
58  
59  
60

1  
2  
3 bohr), for states 1 to 6, respectively. In the first three columns of Table 1 we compare  
4  
5 for each state the computed energy near the minimum positions with the data from  
6  
7 Ref. 9. In the forth and fifth columns of Table 1 we report the computed equilibrium  
8  
9 distance and the corresponding energy. In the last two columns we report the  
10  
11 laboratory data [10]. For states 7B to 12B at 2.0 bohr and for states 13B and 14B at  
12  
13 2.1 bohr the energies (in hartree) are -0.61741, -0.61493, -0.61077, -0.60249, -  
14  
15 0.59530, -0.58116, -0.56447, and -0.54754, respectively. The finding that the minimum  
16  
17 of states 11 to 14 is above the  $H_2^+$  ion energy might be due to the basis set difficulty  
18  
19 to well represent these high states. With the same basis set we obtain for the  $1\sigma_g$  and  
20  
21  $1\sigma_u$  states of the  $H_2^+$  ion, at 2.0 bohr, the energies of -0.602633 and -0.167533  
22  
23 hartree, respectively; both values differ by  $1.5 \times 10^{-6}$  hartree from the best results of  
24  
25 Ref. 11.  
26  
27  
28  
29  
30  
31

32 For very short internuclear distances we report the computed results in Fig. 3.  
33  
34 The PECs of this figure correspond to electronic rather than total energies, for  
35  
36 graphical reasons. The PECs of the top inset accurately merge into the expected  
37  
38 helium excited state energies, as shown in the figure. From  $R=0.01$  to 0.1 bohr the  
39  
40 PECs are obtained from computations with the Helium STO basis set centred midway  
41  
42 the two hydrogen nuclei. From 0.1 to 0.9 bohr, the PECs are more accurately  
43  
44 obtained with the GTO basis set centred on the hydrogen nuclei.  
45  
46  
47  
48

49 In literature the PECs at short distances are often approximated with linear  
50  
51 interpolation from the helium atomic energies with those computed at distances near  
52  
53 1.0 bohr. The data from Fig. 3 indicate that the linear interpolation is reasonable till  
54  
55 about 0.3 bohr; at shorter distances deviations from linearity are noted.  
56  
57  
58  
59  
60

1  
2  
3 For the first 10 states (with energy at the minimum below the  $H_2^+$  ion energy) a tabulation  
4  
5 of the computed energies at selected inter-nuclear distances is provided in Table 2; from  
6  
7  
8  
9  $R=0$  to  $R=0.6$  bohr we have reported the electronic energy, thereafter the total energy.

10  
11  
12  
13  
14  
15 **4. Decomposition into ionic and covalent components.** The Full-CI of HL orbitals  
16  
17 facilitates the decomposition of the total state energies into ionic and covalent  
18  
19 components [1]. In the top inset of Fig. 4 we report for states 1B to 7B both the total  
20  
21 energy and the corresponding covalent component. The covalent component for  
22  
23 states 1B, from  $\sim 2.2$  bohr till dissociation, and for states 3B, and 6B, in the region of  
24  
25 their second minimum, is clearly in need of the ionic component.  
26  
27  
28

29  
30 The state energies for the system  $H^+H^-$  are reported (bullets) in the bottom inset  
31  
32 of Fig. 4. The states are very near in energy to those of  $H_2$  (solid lines), but slightly at  
33  
34 higher energy from short to intermediate distances. The difference between the  $H_2$   
35  
36 and  $H^+H^-$  energies is notable mainly after the first minimum towards large inter-  
37  
38 nuclear distances, around 4-5 bohr, where the  $H^+H^-$  states are experimentally  
39  
40 detected [12]. In this inset we report also the  $H^+H^-$  curve computed with the analytic  
41  
42 expression of Ref. 7, this curve (dashed line) overlaps that of the  $H^+H^-$  ground state  
43  
44 and that of state 6B from 12 bohr till dissociation, for shorter inter-nuclear distances it  
45  
46 is much less attractive. Indeed, from 10 to 12 bohr it overlaps with the curve of state  
47  
48 2B, whereas we find that it is the second excited state of  $H^+H^-$  which overlaps state  
49  
50  
51  
52  
53  
54 2B.

55  
56 As demonstrated by Slater [13], for the  $H_2$  molecule the HL covalent and ionic  
57  
58 functions, though orthogonal at infinity, are highly non-orthogonal at equilibrium and  
59  
60 at shorter distances, actually the shorter the inter-nuclear distance the more the two  
functions resemble one each other. This is not surprising since the two functions must

1  
2  
3 become identical at the united atom. Further, as pointed out by Mulliken [14],  
4  
5 although the excited ionic states are only virtual states for inter-nuclear distances  
6  
7 approaching infinity, at small and intermediate distances the stabilization induced by  
8  
9  $H^+$  on the excited  $H^-$  should convert the virtual states into real states. Indeed, from  
10  
11 Fig. 4 it is evident that for large inter-nuclear distances the PECs of the excited  $H^+H^-$   
12  
13 states are above the dissociation limit, and therefore unstable.  
14  
15

16  
17 Following the  $H_2$  study of Ref. 1, we define the quantity  $\eta$  as the ratio between  
18  
19 the covalent energy component and the total energy,  $\eta = E(\text{covalent})/E(\text{total})$ . This  
20  
21 leads to the definition of the Ionic Energy Percent,  $IEP = 100(1 - \eta)$  also introduced in  
22  
23 Ref. 1. Fig. 5 reports the IEP for the  $^1\Sigma_u^+$  states, in the top insert for the states 1B, 3B  
24  
25 and 6B and in the bottom inset for states 2B, 4B, and 5B. Note that for the latter three  
26  
27 states the IEP is very small and localized, with sharp variations due to state  
28  
29 interactions and state crossing. In addition, whereas for states 3B and 6B the  
30  
31 maximum of IEP occurs at the second minimum position, for state 1B we see an  
32  
33 almost constant contribution from 5 to 8 bohr. The second minimum of state 3B has  
34  
35 been experimentally observed [12, 15], whereas that of state 6B has only been found  
36  
37 from computations [7, 9]. However, unresolved  $H^+H^-$  states above the  $n=4$  threshold  
38  
39 were shown to exist by wave-packets experiments [16].  
40  
41  
42  
43  
44  
45

46  
47 For the  $^1\Sigma_g^+$  states it has been found [1] that for each state manifold dissociating  
48  
49 as  $(1snl)$  with  $n > 1$  there is one state which interacts with the  $H^+H^-$  system leading to  
50  
51 minima at larger and larger inter-nuclear separations the higher the value of  $n$ .  
52  
53 Indeed, a strong ionic character for states EF, H, 7, and 11 was observed. This  
54  
55 finding is here extended to the  $^1\Sigma_u^+$  state manifolds, the states 1B, 3B, 6B and 10B,  
56  
57 all with ionic character, have dissociation limits  $(1s2p)$ ,  $(1s3d)$ ,  $(1s4d)$  and the ion pair  
58  
59  $H^+H^-$ , respectively.  
60

1  
2  
3 By grouping together states with the same  $n$  value in the dissociation products  
4  $H(1s)+H(nl)$ , we obtain the four insets of Fig. 6. For each  $n$  value we report the  $H_2$   
5  
6 states of  $^1\Sigma_g^+$  symmetry (see Ref. 1), those of  $^1\Sigma_u^+$  symmetry, and those of the  $H^+H^-$   
7  
8 system (see Ref. 1). The insets of the figure are complicated because of small energy  
9  
10 differences between states; the figure reveals simply by inspection the complexity of  
11  
12 these “simple” molecular systems. To facilitate the reading of the figure only a few  
13  
14 states are explicitly identified; for example the labels 1g and 1u refer to the first  
15  
16 excited state of symmetry g and u, respectively.  
17  
18  
19  
20  
21  
22  
23  
24  
25  
26

27 **5. Electronic density analysis.** In this section we analyze for each state its orbital  
28  
29 composition at specified inter-nuclear distances, using an analysis based on the  $H_2$   
30  
31 wave functions -obtained with the STO basis sets- equivalent to the atomic radial  
32  
33 distribution function,  $D_{nl}(r)$ ; the details of this comparative analysis are available in  
34  
35 Ref. [1].  
36  
37

38  
39 Since the density in the  $H_2$  molecule is symmetric upon reflexion in the plane  
40  
41 perpendicular to the midpoint of the molecular axis ( $z$  axis), and for any given inter-  
42  
43 nuclear distance the molecular orbitals are linear combinations of STO basis  
44  
45 functions centred at the two nuclear positions, it follows that the knowledge of the  
46  
47 STO linear combination at one nuclear position characterizes the electronic density  
48  
49 also at the other nuclear position. Further for a given state and for a given inter-  
50  
51 nuclear distance,  $R$ , the STO linear combination generally is characterized by  
52  
53 relatively few dominant STO functions.  
54  
55  
56

57  
58 Recall that the radial distribution function for an atom with wave function  $\Psi(r,\theta,\varphi)$   
59  
60 is  $D_{nl}(r) = \Psi^2(r)r^2$  [17]. We introduce a molecular function devised to represent the  
radial distribution function of an atom in a molecule. Specifically for  $H_2$  we consider

1  
2  
3 the electronic density centred on one of the H atoms, set at the origin of the  
4 coordinate system (the other atom being at  $z=-R$ ). For a given *state* of  $H_2$  and at a  
5 given inter-nuclear distance,  $R$ , we compute  $\Psi^2(0,0,z)z^2$  for a set of  $z$  values, in the  
6 interval 0 to infinity. In analogy with the atomic computations of  $D_{nl}(r)$ , we consider the  
7 function  $\Psi^2(0,0,z)z^2$  as a probability distribution function along the  $z$  axis for that H  
8 atom in  $H_2$ . The function is characteristic for a given state and for a given  $R$  value, an  
9 for  $H_2$  is designated as  $D_{\text{state}}(1s, nl)$  or simply "*state*"(1s,  $nl$ ). Clearly at  $R=0$ , the  $D_{nl}(r)$   
10 for a given helium state coincides with "*state*"(1s,  $nl$ ).  
11  
12  
13  
14  
15  
16  
17  
18  
19  
20  
21

22 As reported in Ref. 1, the  $D_{nl}(r)$ s for  $H^-$  are notably different from those of the H or  
23 He atoms and resemble the 1s radial distribution, but with a density nearly node-less  
24 and with a slow decaying toward zero density at large  $r$  values.  
25  
26  
27  
28

29 In the left insets of Fig. 7 we report the plots obtained by adding  $D_{1s}(r)$  to  $D_{nl}(r)$  of  
30 hydrogenic functions. These composed distributions are taken as "reference  
31 distributions" for the dissociation products  $H(1s)+H(nl)$ . In Fig. 7 (right insets) we  
32 report the "*state*"(1s,  $nl$ ) obtained from computations with the STO basis set at the  
33 inter-nuclear distance of 10000 bohr, i.e. at dissociation. Each plot of the radial  
34 distribution functions relates to two orbitals: the 1s orbital generates a peak at very  
35 short distance and the  $nl$  orbital, with  $n = 2$  to 5 and  $l = 0$  to 3, yields the distribution  
36 located at variable distances.  
37  
38  
39  
40  
41  
42  
43  
44  
45  
46  
47

48 In the figure we compare the number of nodes and the positions of the  
49 corresponding maxima (not the intensities) of the  $D_{nl}(r)$  at infinite separation, with  
50 those computed at the inter-nuclear distance  $R=10000$  bohr; for example, the  
51 distribution 6(1s3d) in the left top inset has its counterpart in the distribution 3(1s3d) in  
52 the right top inset. From this comparison, keeping in mind that one hydrogen orbital  
53 is always of 1s type, one can identify the distribution for the other orbital, namely the  
54 orbitals 2p, 2s, 3d, 3p, 3s, 4d, 4f, 4s, 4p, ionic, designated (1s'1s'), 5d, 5s, 5p and 5f,  
55  
56  
57  
58  
59  
60

1  
2  
3 characterizing the states 1B to 14B, respectively. This comparison relates to the  
4  
5 computed dissociation products. Note that the hydrogenic distributions  $D_{nl}(r)$  are  
6  
7 generated orderly, i.e. state 2 corresponds to  $n=2$  and  $l=0$ , state 3 to  $n=2$  and  $l=1$ ,  
8  
9 etc., Further, state 1,  $n=1$  and  $l=0$ , is omitted since no  $^1\Sigma_u^+$  state dissociates as  
10  
11  $H(1s)+H(1s)$ . For the computed distributions on the left insets, the sequence of the  
12  
13 integers 1, 2, 3, ... represents the order of the roots obtained from the diagonalization  
14  
15 of the secular equation, thus the state order is assigned unambiguously.  
16  
17  
18  
19

20  
21 In Fig. 8 we report the radial distribution functions for states 1B to 9B at the  
22  
23 internuclear distances of 0.5 bohr (i.e. approaching the helium united atom) and 2.0  
24  
25 bohr, the distance near the first minimum for most states (see Table 1). The  
26  
27 symmetry of the system imposes that at the united atom the state configurations are  
28  
29 restricted to (1snp) and (1snf). In Fig. 8 the radial distribution functions at 0.5 bohr  
30  
31 respect this symmetry constraint. However, at the united atom, the states (1snp) and  
32  
33 (1snf) are known to be nearly degenerate [18] with the energies of the states (1snf)  
34  
35 slightly lower than those of the states (1snp). Computationally, we correctly obtain the  
36  
37 two states very close in energy, but our hydrogen basis set yields the energy of the  
38  
39 states (1snp) slightly lower than that of the states (1snf). Therefore, approaching the  
40  
41 united atom state crossings, not detected by our computations, are expected between  
42  
43 the pairs of states 3 and 4, 5 and 6, 7 and 9.  
44  
45  
46  
47

48  
49 From the right insets of Fig. 8, at the internuclear distance of 2.0 bohr, we see a  
50  
51 variety of state configurations. The configuration of 1B is a mixture of the ionic (1s'1s')  
52  
53 with the (1s2p) configurations, then the configurations (1snp) at 0.5 bohr switch to  
54  
55 (1snd) at 2.0 bohr.  
56  
57

58  
59 We have computed the radial distribution functions for each state at 19 inter-  
60  
nuclear separations, starting at  $R=0.5$  bohr and ending at 100 bohr; the density at

1  
2  
3 dissociation is analyzed twice, at  $R=1000$  and  $10000$  bohr, as for the  $^1\Sigma_g^+$  states [1],  
4  
5  
6 the two computations yield the same results.  
7

8  
9 The 1B state from dissociation to about  $15$  bohr has the electronic configuration  
10  
11  $(1s2p)$ , which becomes ionic  $(1s'1s')$  till  $2.2$  bohr, and at  $2.0$  it becomes a mixture of  
12  
13  $(1s'1s')$  and  $(1s2p)$  till it merges into the united atom configuration  $\text{He}(1s2p)$ . The  
14  
15 relative importance of ionic and covalent components for this state has been  
16  
17 discussed by Kolos [3] and Mulliken [14]. The electronic configurations at the united  
18  
19 atom, at dissociation and at intermediate inter-nuclear distances are in agreement  
20  
21 with those proposed by Mulliken [14].  
22  
23

24  
25 The 2B state configuration from dissociation to about  $5.0$  bohr is  $(1s2s)$ ; from  $2.5$   
26  
27 bohr to  $2.0$  becomes  $(1s3d)$ , then  $(1s3p)$  till it merges into  $\text{He}(1s3p)$ . Again, in  
28  
29 agreement with Mulliken [14].  
30

31  
32 The state 3B configuration from dissociation to  $\sim 100$  bohr is  $(1s3d)$  then it  
33  
34 becomes the ionic configuration  $(1s'1s')$  till  $5.7$  bohr where there is a mixture of the  
35  
36 ionic and  $(1s2s)$  configurations. From  $5.4$  to  $5.0$  bohr it is  $(1s3p)$ ; from  $2.5$  to  $2.0$  bohr  
37  
38 it becomes  $(1s4d)$  and from  $1.0$  to  $0.5$  bohr  $(1s4p)$  merging into the united atom  
39  
40  $\text{He}(1s4f)$ .  
41  
42

43  
44 The state 4B configuration from dissociation to  $6.2$  bohr is  $(1s3p)$ . From  $5.7$  to  $5.4$   
45  
46 bohr it is a mixture of ionic and  $(1s3l)$  likely  $(1s3s)$ ; this is the region of an avoided  
47  
48 state crossing with the 3B state. As shown in the bottom inset of Fig. 4 the ionic state  
49  
50 3 of  $\text{H}^+\text{H}^-$  overlaps with state 4B between  $5.4$  and  $6$  bohr. At  $5.0$  bohr the 4B  
51  
52 configuration is  $(1s3d)$  and from  $2.5$  to the united atom it becomes  $(1s4l)$  first  $4d$ , till  
53  
54  $2.0$  bohr, then  $4f$  in approaching the united atom, rather than  $(1s4p)$ .  
55  
56

57  
58 The state 5B configuration from dissociation to  $6.2$  bohr is  $(1s3s)$ , from  $5.7$  to  $5.0$   
59  
60 bohr is  $(1s4d)$ ; then from  $2.5$  to  $0.5$  bohr it becomes  $(1s5l)$  first  $(1s5d)$  till  $1.0$  bohr,  
then  $(1s5p)$  rather than  $(1s5f)$ , the united atom.

1  
2  
3 The state 6B configuration at infinity is (1s4d), but it becomes ionic from 100 to 15  
4 bohr; from 15 to 5.0 bohr is (1s3l) mainly (1s3s), and from 2.5 to the united atom it is  
5 (1s5f) rather than (1s5p), the united atom configuration.  
6  
7

8  
9  
10 The state 7B configuration at dissociation is (1s4f), but it becomes (1s4d) at 100  
11 bohr, and (1s4f) from 34 bohr to 10 bohr, then (1s4p) from 6.2 to 5.7 bohr and (1s5f)  
12 at 5 bohr. From 2.5 bohr to the united atom the configuration is (1s6l), specifically  
13 (1s6d) till 2.0 and then (1s6p); the united atom is He(1s6f).  
14  
15

16  
17  
18 The state 8B configuration at dissociation is (1s4s); from 20 to 15 it is (1s4d), at  
19 10 bohr it is (1s4s); from 6.2 to 5.4 bohr it is (1s5f), from 2.5 to the united atom it  
20 becomes (1s6l) mainly (1s6f); the united atom is He(1s6p).  
21  
22

23  
24  
25 The state 9B configuration from dissociation to 10 bohr is (1s4p); from 6.2 to 5.0  
26 bohr it is (1s5l) first (1s5f), then (1s5p) and finally (1s5s); from 2.5 bohr to the united  
27 atom it becomes (1s7l) first (1s7d) till 2.0 bohr then (1s7p); the united atom is  
28 He(1s7f).  
29  
30

31  
32  
33 State 10B dissociates as  $H^+H^-$ . From 100 to 10 bohr the configuration is (1s4l),  
34 starting with (1s4s). At 6.2 bohr it becomes (1s5p); from 5.7 to 5.0 bohr it is (1s6l);  
35 from 2.5 to 2.0 bohr it is (1s8p) then switches to (1s7f) till the united atom, which is  
36 He(1s7p).  
37  
38

39  
40  
41 States 11B, 12B, 13B and 14B dissociate as (1s5d), (1s5s), (1s5p) and (1s5f),  
42 respectively; the corresponding states at the united atom are He(1s8f), He(1s8p),  
43 He(1s9f), and He(1s9p). The radial densities for these states are characterized by  
44 many nodes, therefore not easily classifiable.  
45  
46

47  
48  
49 **6. Basis sub-set decompositions.** The identification of the electronic configurations  
50 obtained in the previous section is confirmed by decomposing the STO basis set into  
51 sub-sets with the same  $l$  value (for example all the  $ns$  STO, or all the  $np$  STO, etc.)  
52  
53  
54  
55  
56  
57  
58  
59  
60

1  
2  
3 These sub-sets bring specific and characteristic contributions to the total energy of  
4 the 1B to nB states and thus to the corresponding electronic density. The results of  
5 this analysis are summarized in Figs. 9 and 10.  
6  
7  
8  
9

10 The top left inset of Fig. 9 reports computations of the B states using only *ns* STO  
11 (dashed curves) to be compared with thin lines (full curves) representing the final  
12 computations previously reported in Fig. 2. With the *ns* sub-set only the 1B and the  
13 2B state are crudely reproduced, indicating a strong *ns* contribution for these states.  
14  
15 The curve 1a and, starting from ~3 bohr till dissociation, the 2a are formed by the 2s  
16 functions. The 3s functions generate the first minimum of curve 2a and, starting from  
17 3 bohr till dissociation the two curves 3a and 4a which cross in the region 6-7 bohr.  
18  
19 The state crossing at ~5.3 bohr between curves 5a and 6a is generated by the 4s  
20 functions. The first cross, between 3a and 4a, is retained in the final PECs, the  
21 second one resolves into a pronounced bump for state 5B. At this level, the dashed  
22 PECs for the 3B, 4B and 5B states are clearly incorrectly reproduced, indicating the  
23 need of STO of higher *l* values.  
24  
25  
26  
27  
28  
29  
30  
31  
32  
33  
34  
35  
36  
37

38 Indeed, proceeding to the top right inset, one can see that the combined *ns* and  
39 2p STO sub-sets are capable to reproduce, although with different accuracy, the  
40 states 1B, 2B, 3B, 4B and, only approximately, 5B. The avoided state crossings  
41 between curves 3a and 4a and between 5a and 6a are now more evident. Further,  
42 from the figure we learn that most of the 2p effect is due to 2p<sub>σ</sub> functions (thick full  
43 lines) with limited contribution from the 2p<sub>π</sub> (dashed lines), important only for the 1a  
44 and 3a curves. Addition of the full *np* sub-set improves the accuracy which is now  
45 acceptable for the states 1B, 2B and 3B.  
46  
47  
48  
49  
50  
51  
52  
53  
54  
55  
56

57 Addition of the *nd* STO sub-set notably improves the energy for all the states  
58 dissociating up to 1s+4*l*. For the higher states the representation is poor. These  
59 graphs are overcrowded, thus not easily readable, but provide a synthetic and over-  
60

1  
2  
3 all summary on the effect of the different sub-sets of STO, and confirm the density  
4 analysis conclusions.  
5  
6

7  
8 The graphs reported in the insets of Fig. 10 confirm clearly and in detail the  
9 conclusions above obtained for the states 1B to 8B . From this figure we note that for  
10 the 1B, 2B and 3B states large energy improvements are mainly due to  $2p_{\sigma}$  STO. For  
11 the state 4B the  $3p_{\sigma}$  is dominant among the  $np_{\sigma}$  STO; for states 5B to 8B the STO  
12  $3p_{\sigma}$ ,  $4p_{\sigma}$ , and  $5p_{\sigma}$  become dominant. The need of inclusion of the  $nd$  STO becomes  
13 apparent starting from state 5B till state 8B. The need of  $nf$  STO is clearly noted for  
14 State 8B.  
15  
16  
17  
18  
19  
20  
21  
22  
23

24 This state by state energy decomposition analysis confirms the previous deductions  
25 on the main contribution by specific  $nl$  orbitals for the  $^1\Sigma_u^+$  states.  
26  
27  
28  
29  
30  
31

32 **7. Conclusions.** The  $^1\Sigma_u^+$  state computations reported in this work are performed with  
33 extended and optimized STO and GTO basis sets. The energies of the 1B to 6B  
34 states are in nice agreement with the accurate computations by Wolniewicz *et al.* [9]  
35 and slightly better than those reported in Ref. [7].  
36  
37  
38  
39  
40  
41

42 The evolution of the electronic density is analyzed in detail state by state with the  
43 comparative probability density analysis, and by a study of the relative importance of  
44 basis sub-sets. The computations for states 6B to 9B complete for the first time the  
45 manifold of states dissociating as  $H(1s) + H(4l)$ . For the state manifold dissociating  
46 into  $H(1s) + H(5l)$  the computations reported are less reliable, due to limitations in the  
47 basis sets for high  $n$  and  $l$  values; however, we find that these states dissociate  
48 correctly and all, but B10, have minima lying just above the  $1\sigma_g$  state of the  $H_2^+$   
49 system.  
50  
51  
52  
53  
54  
55  
56  
57  
58  
59  
60

1  
2  
3  
4 The ionic character of the  $^1\Sigma_u^+$  states is quantitatively determined. For states  
5  
6 dissociating as  $(1snl)$  a rule has been noted: for each  $n>1$  value there is one state  
7  
8 which strongly interacts with the  $H^+H^-$  system leading to minima with ionic character at  
9  
10 larger and larger inter-nuclear separations the higher the value of  $n$ . This rule,  
11  
12 previously found for the  $^1\Sigma_g^+$  state is here extended to the  $^1\Sigma_u^+$  states. In both case,  
13  
14 the first state of the  $(1s5l)$  manifold dissociates as  $H^+H^-$ .  
15  
16  
17  
18  
19

20 **8. Acknowledgement.** One of us (G.C.) acknowledges a grant from MIUR-  
21 2006030944.  
22  
23  
24  
25  
26  
27  
28  
29  
30  
31  
32  
33  
34  
35  
36  
37  
38  
39  
40  
41  
42  
43  
44  
45  
46  
47  
48  
49  
50  
51  
52  
53  
54  
55  
56  
57  
58  
59  
60

**References.**

1. Corongiu, G.; Clementi, E. *J. Chem. Phys.* **2009** (in press).
2. Kolos, W.; Wolniewicz, L. *J. Chem. Phys.* **1965**, *43*, 2429.
3. Kolos, W.; Wolniewicz, L. *J. Chem. Phys.* **1966**, *45*, 509.
4. Rothenberg, S.; Davidson, E. R. *J. Chem. Phys.* **1966**, *45*, 2560.
5. Kolos, W. *J. Mol. Spectrosc.* **1976**, *62*, 429.
6. Dressler, K.; Wolniewicz, L. *Ber. Bunsenges. Phys. Chem.* **1995**, *99*, 246.
7. Detmer, T.; Schmelcher, P.; Cederbaum, L. S. *J. Chem. Phys.* **1998**, *109*, 9694.
8. de Lange, A.; Hogervorst, W.; Ubachs, W.; Wolniewicz, L. *Phys. Rev. Lett.* **2001**, *86*, 2988.
9. Staszewska, G.; Wolniewicz, L. *J. Mol. Spectrosc.* **2002**, *212*, 208.
10. Huber, K. P.; Herzberg, G. *Molecular Spectra and Molecular Structure IV. Constants of Diatomic Molecules*, Van Nostrand Reinhold, New York, **1979**.
11. Ishikawa, A.; Nakashima, H.; Nakatsuji, H. *J. Chem. Phys.* **2008**, *128*, 124103.
12. Vieitez, M. O.; Ivanov, T. I.; Reinhold, E.; de Lange, C. A.; Ubachs, W. *Phys. Rev. Letters* **2008**, *101*, 163001.
13. Slater, J. C. *J. Chem. Phys.* **1951**, *19*, 220.
14. Mulliken, R. S. *J. Am. Chem. Soc.* **1966**, *88*, 1849.
15. Koelemeij, J. C. J.; de Lange, A.; Ubachs, W. *Chem. Phys.* **2003**, *287*, 349.
16. Reinholds, E.; Ubachs, W. *Mol. Phys.* **2005**, *103*, 1329.
17. Pauling, L.; Wilson, E. B. *Introduction to Quantum Mechanics*, Mc Graw-Hill, Book Company, New York, **1935**.
18. Moore, C. E. *Atomic Energy Levels*, Vol. 1, NBS Circular 467, U. S. Government Printing Office, Washington D.C., Dec. **1971**.

**Table 1.** Comparison of total energies,  $E$  (hartree), near the minimum positions,  $R$  (bohr), from Wolniewicz data [9] and from this work. Computed equilibrium distance,  $R_{\text{eq}}$  (bohr), and energy,  $E_{\text{eq}}$  (hartree), from this work. The last two columns,  $R(\text{exp})$  and  $E(\text{exp})$  are laboratory data [10].

State	$R$	$-E$ (Ref. 9)	$-E$ (this work)	$R_{\text{eq}}$	$-E_{\text{eq}}$	$R(\text{exp})$	$-E(\text{exp})$
1B	2.4	0.756674	0.75652	2.420	0.75653	2.4431	0.75666 0
2B	2.1	0.665791	0.66576	2.085	0.66577	2.1150	0.66579 3
3B	2.0	0.636960	0.63695	2.032	0.63698	2.1161	0.63689 9
3B	11.1	0.605666	0.60551	11.12	0.60551	--	--
4B	2.0	0.634102	0.63409	2.000	0.63409	--	--
5B	2.0	0.624204	0.62419	2.012	0.62419	--	--
6B	2.0	0.622749	0.62271	1.998	0.62272	--	--
6B	34.0	0.555504	0.55548	33.80	0.55548	--	--

**Table 2.** Energy values (hartree) at inter-nuclear distances, R (bohr), for states 1 to 10.

R

No	0.00	0.01	0.02	0.20	0.40	0.60	0.80	1.00	1.20	1.40	1.60
1	-2.12376	-2.12350	-2.12272	-2.05257	-1.92533	-1.79716	-0.43179	-0.58129	-0.66127	-0.70570	-0.73069
2	-2.05512	-2.05485	-2.05408	-1.98377	-1.85610	-1.72716	-0.36064	-0.50861	-0.58663	-0.62867	-0.65084
3	-2.03125	-2.03099	-2.03021	-1.95983	-1.83199	-1.70277	-0.33598	-0.48357	-0.56111	-0.60256	-0.62403
4	-2.03101	-2.03075	-2.02997	-1.95967	-1.83189	-1.70275	-0.33576	-0.48309	-0.56030	-0.60133	-0.62232
5	-2.02000	-2.01974	-2.01896	-1.94855	-1.82070	-1.69149	-0.32460	-0.47205	-0.54942	-0.59066	-0.61187
6	-2.01982	-2.01955	-2.01878	-1.94849	-1.82068	-1.69145	-0.32446	-0.47178	-0.54898	-0.59000	-0.61097
7	-2.01317	-2.01290	-2.01213	-1.94233	-1.81451	-1.68530	-0.31836	-0.46577	-0.54307	-0.58422	-0.60534
8	-2.00991	-2.00965	-2.00887	-1.94070	-1.81289	-1.68366	-0.31667	-0.46399	-0.54119	-0.58222	-0.60319
9	-1.98096	-1.98069	-1.97991	-1.93465	-1.80683	-1.67764	-0.31078	-0.45829	-0.53573	-0.57705	-0.59834
10	-1.96187	-1.96160	-1.97604	-1.92796	-1.80017	-1.67096	-0.30398	-0.45131	-0.52854	-0.56960	-0.59062

R

No	1.70	1.90	2.00	2.10	2.20	2.40	2.80	3.00	3.20	3.60	4.00
1	-0.73867	-0.74888	-0.75196	-0.75408	-0.75544	-0.75652	-0.75456	-0.75234	-0.74957	-0.74291	-0.73526
2	-0.65727	-0.66414	-0.66545	-0.66576	-0.66530	-0.66274	-0.65425	-0.64946	-0.64481	-0.63680	-0.63129
3	-0.63007	-0.63609	-0.63695	-0.63679	-0.63584	-0.63227	-0.62163	-0.61570	-0.60983	-0.59906	-0.59014
4	-0.62810	-0.63354	-0.63409	-0.63362	-0.63235	-0.62812	-0.61605	-0.60935	-0.60263	-0.58987	-0.57869
5	-0.61778	-0.62350	-0.62419	-0.62387	-0.62275	-0.61882	-0.60741	-0.60106	-0.59473	-0.58288	-0.57269
6	-0.61674	-0.62217	-0.62271	-0.62223	-0.62094	-0.61669	-0.60457	-0.59782	-0.59106	-0.57818	-0.56684
7	-0.61119	-0.61678	-0.61741	-0.61701	-0.61582	-0.61174	-0.60000	-0.59345	-0.58691	-0.57457	-0.56381
8	-0.60896	-0.61439	-0.61493	-0.61444	-0.61316	-0.60890	-0.59676	-0.59001	-0.58325	-0.57038	-0.55907
9	-0.60427	-0.61005	-0.61077	-0.61046	-0.60935	-0.60544	-0.59398	-0.58756	-0.58114	-0.56898	-0.55829
10	-0.59642	-0.60191	-0.60249	-0.60204	-0.60079	-0.59663	-0.58473	-0.57812	-0.57151	-0.55911	-0.54933

R

No	4.40	4.80	5.20	5.60	5.80	6.40	7.00	7.60	8.00	9.00	10.00
1	-0.72711	-0.71877	-0.71048	-0.70240	-0.69848	-0.68729	-0.67706	-0.66783	-0.66222	-0.65011	-0.64054
2	-0.62826	-0.62692	-0.62644	-0.62630	-0.62628	-0.62621	-0.62610	-0.62596	-0.62586	-0.62565	-0.62548
3	-0.58289	-0.57681	-0.57168	-0.56781	-0.56869	-0.57593	-0.58290	-0.58907	-0.59266	-0.59965	-0.60390
4	-0.56961	-0.56344	-0.56231	-0.56547	-0.56517	-0.56119	-0.55863	-0.55724	-0.55672	-0.55612	-0.55589
5	-0.56422	-0.55734	-0.55240	-0.55023	-0.55025	-0.55177	-0.55321	-0.55420	-0.55465	-0.55529	-0.55552
6	-0.55753	-0.55132	-0.54858	-0.54572	-0.54447	-0.54194	-0.54127	-0.54122	-0.54113	-0.54066	-0.54036
7	-0.55484	-0.54796	-0.54436	-0.54293	-0.54171	-0.53782	-0.53509	-0.53348	-0.53282	-0.53201	-0.53170
8	-0.54995	-0.54416	-0.53965	-0.53541	-0.53358	-0.53097	-0.53187	-0.53173	-0.53158	-0.53145	-0.53141
9	-0.54928	-0.54240	-0.53847	-0.53439	-0.53247	-0.52928	-0.52841	-0.52957	-0.53010	-0.53087	-0.53115
10	-0.54239	-0.53826	-0.53349	-0.52888	-0.52734	-0.52807	-0.52689	-0.52576	-0.52532	-0.52432	-0.52380

R

No	11.00	11.10	12.00	13.00	20.00	30.00	34.00	40.00	50.00	100	10000
1	-0.63358	-0.63303	-0.62921	-0.62697	-0.62514	-0.62504	-0.62503	-0.62502	-0.62501	-0.62500	-0.62500
2	-0.62536	-0.62535	-0.62527	-0.62519	-0.62500	-0.62500	-0.62500	-0.62500	-0.62500	-0.62500	-0.62500
3	-0.60549	-0.60551	-0.60461	-0.60187	-0.57827	-0.56109	-0.55711	-0.55556	-0.55555	-0.55555	-0.55555
4	-0.55578	-0.55578	-0.55572	-0.55567	-0.55557	-0.55555	-0.55555	-0.55554	-0.55554	-0.55554	-0.55554
5	-0.55559	-0.55559	-0.55559	-0.55558	-0.55554	-0.55553	-0.55553	-0.55553	-0.55553	-0.55552	-0.55552
6	-0.54048	-0.54053	-0.54118	-0.54244	-0.55281	-0.55542	-0.55548	-0.55261	-0.54758	-0.53756	-0.53122
7	-0.53159	-0.53158	-0.53153	-0.53147	-0.53126	-0.53122	-0.53122	-0.53121	-0.53122	-0.53122	-0.53120
8	-0.53138	-0.53137	-0.53134	-0.53131	-0.53120	-0.53117	-0.53117	-0.53118	-0.53120	-0.53120	-0.53114
9	-0.53124	-0.53124	-0.53124	-0.53123	-0.53117	-0.53104	-0.53104	-0.53111	-0.53115	-0.53114	-0.53056
10	-0.52361	-0.52362	-0.52382	-0.52432	-0.52559	-0.52934	-0.53030	-0.53074	-0.53069	-0.53058	-0.52766

Figure 1. State diagram for the  $1\Sigma_u^+$  excited states 1 to 9 of the  $H_2$  molecule.

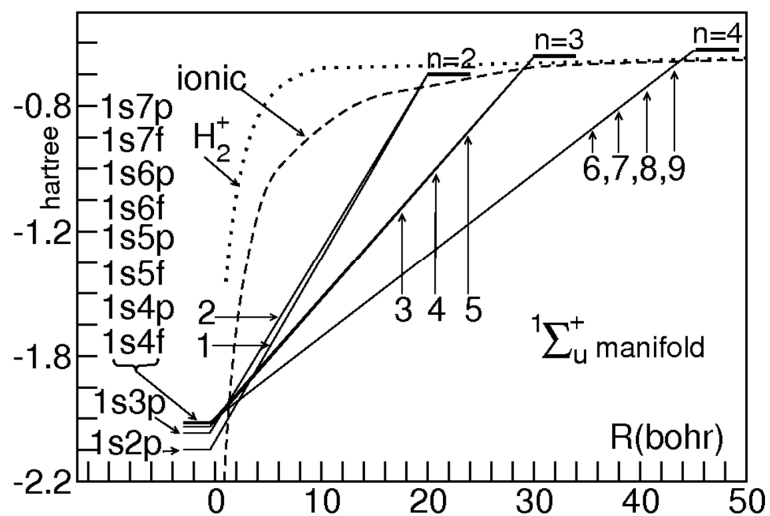
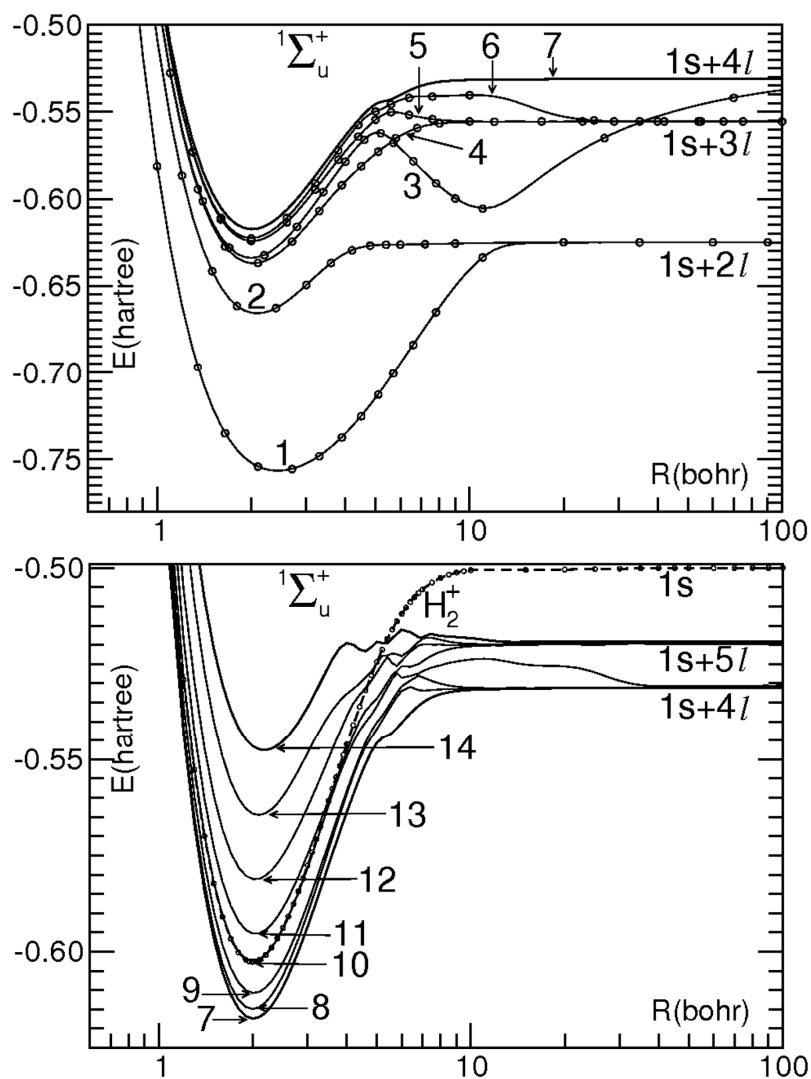
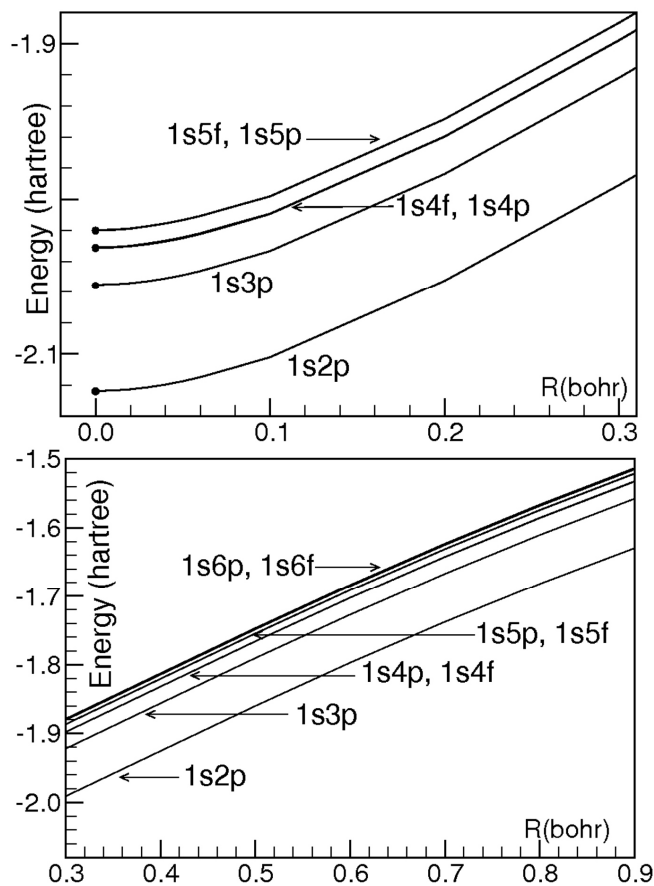


Figure 2. PECs for the  $^1\Sigma_u^+$  excited states of the  $H_2$  molecule.



**Figure 3.** Short distance electronic energies. Top: from the united atom ( $R=0$ ) to 0.3 bohr. Bottom: from 0.3 to 0.9 bohr.



**Figure 4.** Top: total and corresponding covalent energy component for the states 1 to 7. Bottom: energies for the system  $H^+H^-$ .

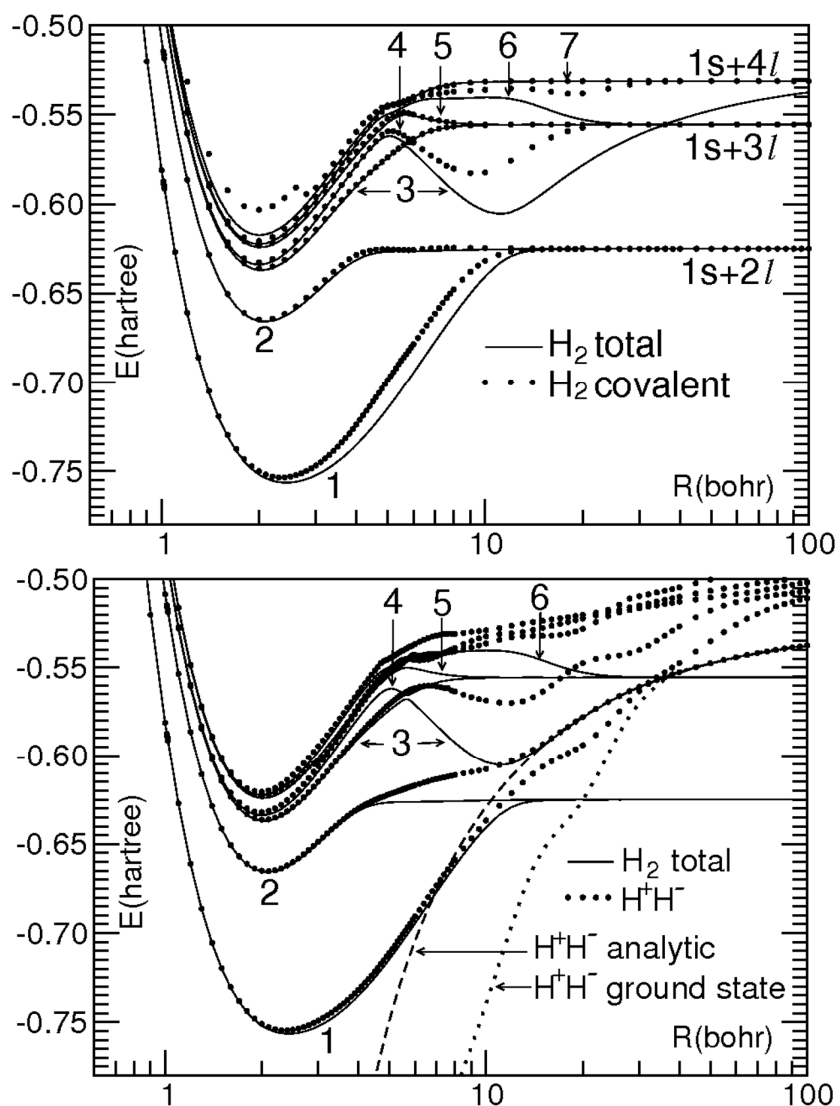


**Figure 5.** IEP for the  $^1\Sigma_u^+$  states. Top: for 1B, 3B and 6B states. Bottom: for 2B, 4B, and 5B.

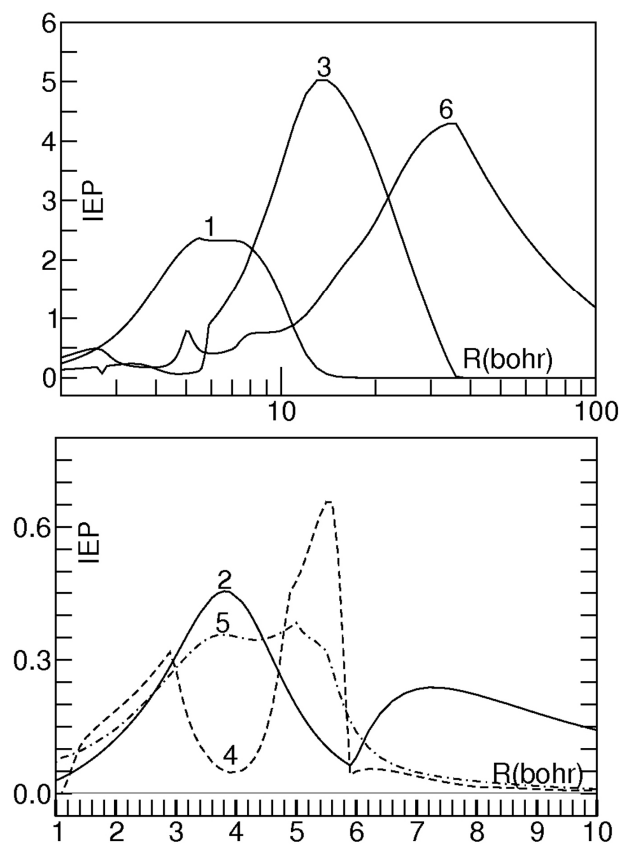


**Figure 6.** PECs for the  $1\Sigma_g^+$  states (dashed lines),  $1\Sigma_u^+$  states (full lines) in the  $H_2$  molecule, and for the  $H^+H^-$  (full line with bullets).

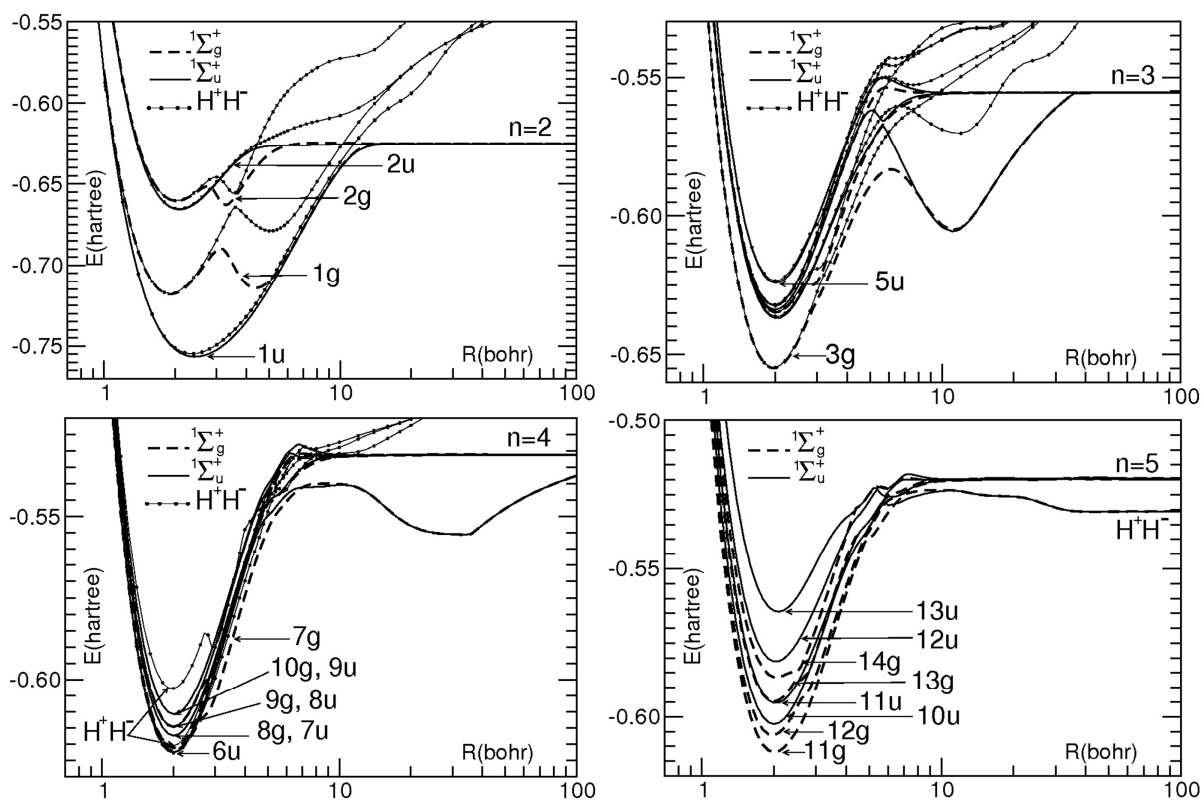


**Figure 7.** Right: plots of  $D_{1s}(r) + D_{nl}(r)$  radial distributions of hydrogenic orbitals. Left: plot of “state”(1s, $nl$ )( $r$ ), with  $n=1$  to 5, for  $H_2$  at the inter-nuclear distance  $R=10000$  bohr.

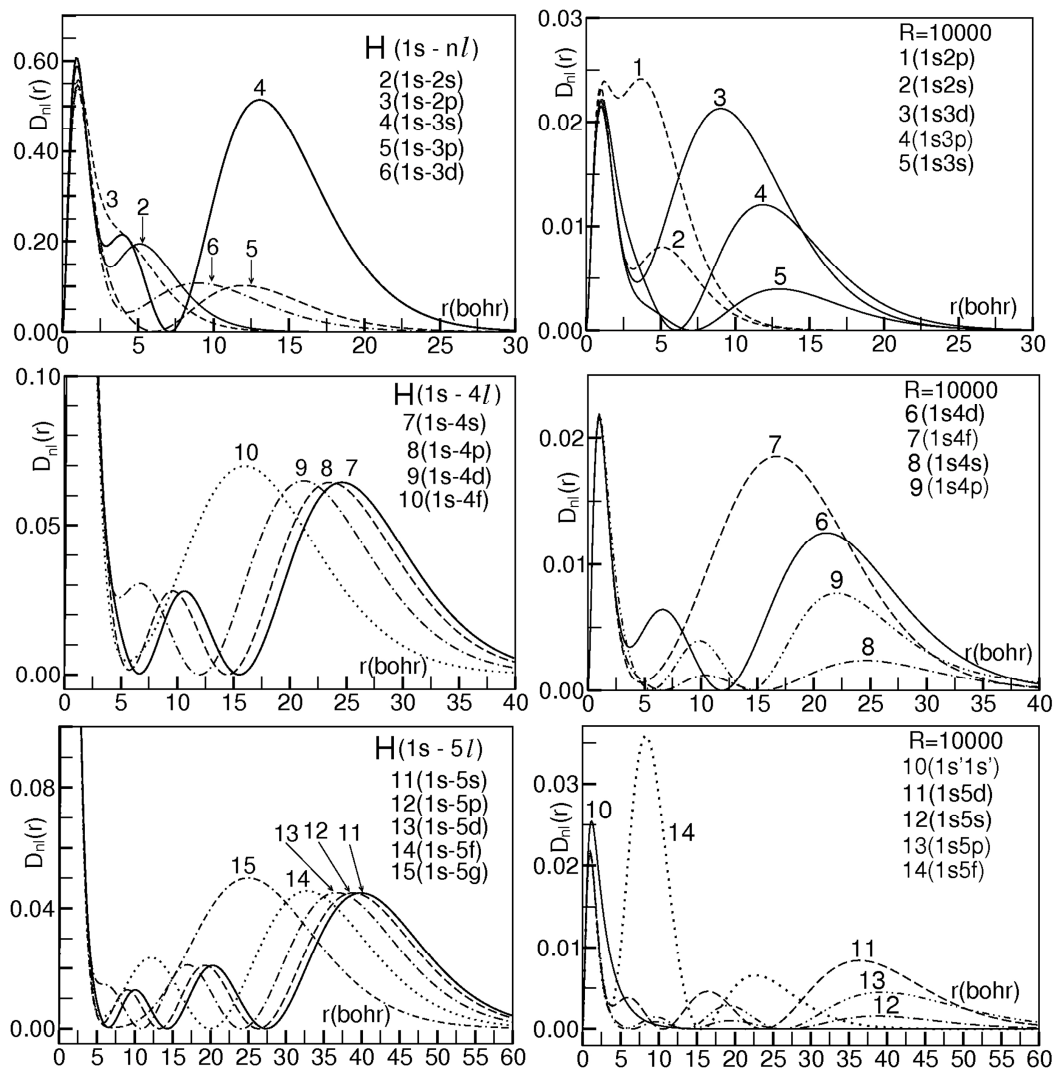


**Figure 8.** Plots of “state”(1s,nl)(r) for states 1 to 9. Right: at the inter-nuclear distance R=0.5 bohr, left: at R=2.0 bohr.

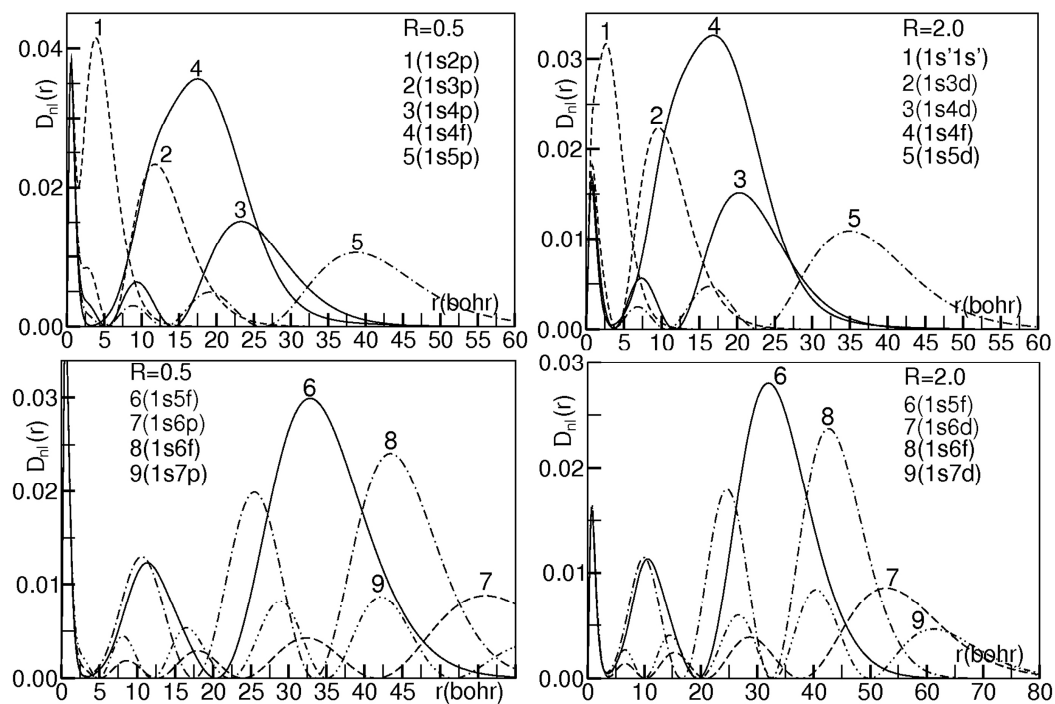


**Figure 9.** PECs computed with STO sub-sets (dashed curves) and full STO basis set (thin full curves).

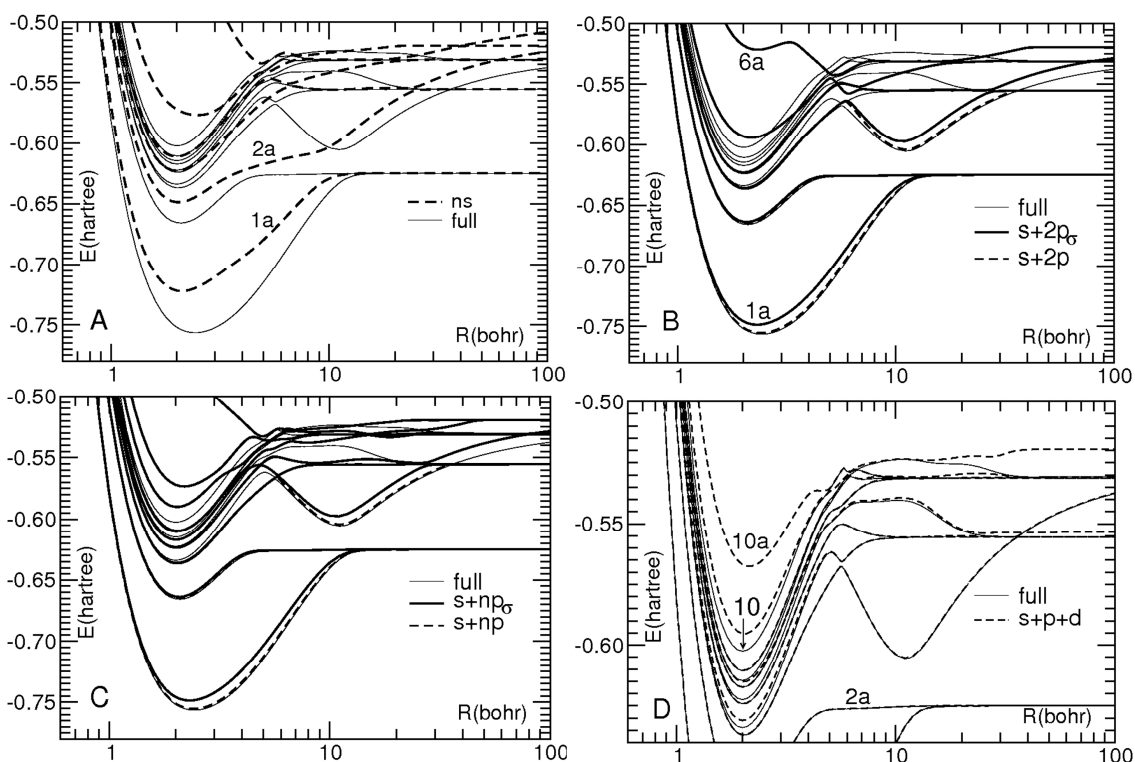


**Figure 10.** PECs for states 1 to 8 obtained from  $ns$  STO sub-sets to full STO basis set.

